

Electrochemical Scanning Tunneling Spectroscopy of Redox-Active Molecules Bound by Au–C Bonds

Alejandra M. Ricci,[†] Ernesto J. Calvo,^{*,†} Santiago Martin,[‡] and Richard J. Nichols[‡]

INQUIMAE, Facultad de Ciencias Exactas y Naturales, Universidad de Buenos Aires, Pabellón 2, Ciudad Universitaria, Buenos Aires CP 1428, Argentina, and Department of Chemistry and Centre for Nanoscale Science, University of Liverpool, Liverpool L69 7ZD, U.K.

Received September 16, 2009; E-mail: calvo@qi.fcen.uba.ar

In recent years it has become possible to measure the electrical and electrochemical behavior of small numbers of molecules, with even the single-molecule limit being achieved.^{1–4} This has enabled systematic investigation of the influence of molecular structure as well as contact and environmental factors on the conductance of molecular electronic junctions.⁵ Such molecular junctions have most frequently employed Au leads, although other contacts such as Pt⁶ and indium tin oxide⁷ have been used. Molecules have typically been bound in such junctions using “conventional” chemisorption chemistry, employing, for instance, thiolate, amine, phosphine, pyridyl, or nitrile end groups for binding to the metal contacts.^{4,8} Electrical measurements on thiolate contacts have highlighted potential inadequacies in such contacting strategies, including high apparent contact resistance, mobility of chemisorbed contacts at ambient temperatures, and stochastic switching of the junction conductance.⁹ Direct metal–carbon (M–C) bonding offers an attractive alternative¹⁰ and is indeed a feature of well-contacted carbon nanotubes.¹¹ Chemical strategies for directly contacting organic molecules and redox-active molecules through M–C bonds have been devised.¹² However, the electrical properties of such M–C-linked molecular wires remain largely unexplored. Here we report on a pair of redox-active molecular wires, one linked to the Au(111) surface contact through thiolate and the other directly linked through M–C bonding. Electrochemical scanning tunneling spectroscopy has been used to address these systems, and we present the first report on electrochemically gated electron transfer (ET) using a M–C-contacted molecule.

Figure 1 shows the redox-active [Os(bipyridine)(pyridine)Cl] complex studied. The same redox molecular structure was tethered by two different strategies, namely, via mercaptobenzoic acid or reduction of the aryldiazonium salt of *p*-aminobenzoic acid, resulting in either Au–S or Au–C bonds, respectively. The electrochemical scanning tunneling microscopy (STM) configuration was used to study charge transport through the redox center and determine whether the electrochemical potential can be used to regulate (“gate”) ET across the molecule with either the Au–C-contacted molecule or the more conventional Au–S bonding. In the most common electrochemical STM spectroscopy (EC-STs) arrangement, the electrochemical potential is swept while keeping the tip-to-sample bias and distance constant.¹³ This is a four-electrode configuration, and changes in the electrochemical potential alter the relative energetic positions of the metal-contact Fermi energy and the molecular electronic levels of the redox group. This has been called the molecular electrochemical transistor configuration, where the reference (or counter) electrode is considered as the gate, the STM tip as the source, and the substrate as the drain. Such configurations have been used to study ET through

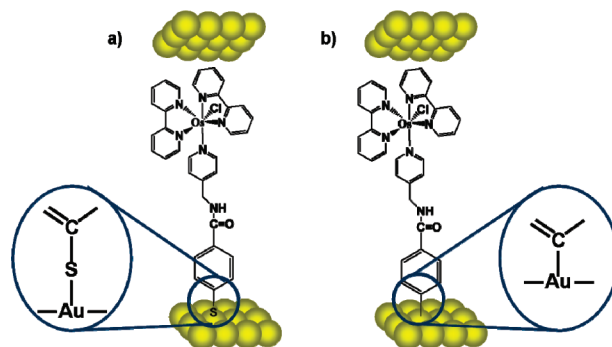


Figure 1. Schematic structures of the [Os(bipyridine)(pyridine)Cl] complexes in the tunneling gap, tethered to the surface by (a) S and (b) C as the anchoring atoms.

iron protoporphyrin IX,¹ Os and Co complexes,^{13,14} and viologens.¹⁵ Such experiments have been interpreted within theoretical frameworks previously developed for in situ STM processes of redox molecules.¹⁶

The adsorbed layers shown in Figure 1 were formed as described in the Supporting Information (SI). We will refer to the S- and C-anchored systems as Au(111)/SPhCOOH/Os and Au(111)/PhCOOH/Os, respectively. The EC-STs measurements are described in the SI. Briefly, the set-point current was 1 nA, and the bias potential between the tip (T) and substrate (S), $E_{\text{bias}} = E_{\text{T}} - E_{\text{S}}$, was kept constant. The initial substrate electrochemical potential ($E_{\text{S,i}}$) was set suitably away from the equilibrium redox potential of the complex (E°). At this point, the feedback loop was switched off, and the substrate potential (E_{S}) was scanned in a potential window wide enough to pass E° with both E_{S} and the tip potential E_{T} while the current flowing through the molecular junction (I_{T}) was monitored.

Figure 2 depicts typical I_{T} versus $(E_{\text{S}} - E^{\circ})$ curves for the Os complex tethered to the Au surface by Au–C (Figure 2a) and Au–S (Figure 2b) bonds, both recorded at $E_{\text{bias}} = +0.05$ V. The curves exhibit I_{T} maxima at $E_{\text{max}} = 0.04$ and 0.1 V for the Au–C and Au–S bonds, respectively, in the positive-going potential scan. For comparison, the corresponding cyclic voltammograms (CVs) are also displayed;¹⁷ they show that E_{max} is close to the equilibrium redox potential of the complex. Notably, approximately the same initial I_{T} was reached at $(E_{\text{S}} - E^{\circ}) = 0.2$ V, indicating close to constant tip-to-sample height during the full E_{S} sweep. For the fully reduced [$(E_{\text{S}} - E^{\circ}) = -0.2$ V] and fully oxidized [$(E_{\text{S}} - E^{\circ}) = 0.2$ V] Os complexes tethered to the surface, the tunneling current reached a minimum of ~ 1 nA, while a pronounced maximum current at E_{max} of 2–3 nA was observed. This points to the participation of the Os complex in the ET mechanism for both the S and C surface-tethered species.

These results are consistent with the predictions of the two-step ET model with partial vibrational relaxation at the redox center

[†] Universidad de Buenos Aires.

[‡] University of Liverpool.

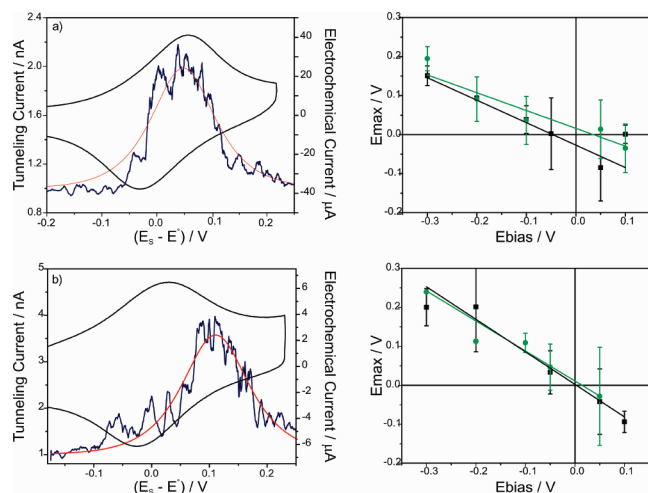


Figure 2. Plots of I_T vs $E_S - E^\circ$ (positive-going sweep) recorded in 0.1 M KClO₄ with $E_{bias} = +0.05$ V for (a) Au(111)/PhCOOH/Os and (b) Au(111)/SPhCOOH/Os (blue lines, left scale). The red lines correspond to the best fits of I_T to eq 1. The CVs (in 0.1 M NaClO₄, 500 mV s⁻¹) are also shown (black lines, right scale). Corresponding plots of E_{max} (the peak position in I_T) vs E_{bias} are also shown to the right; ● and ■ symbols denote anodic and cathodic scans, respectively.

developed by Ulstrup, Kuznetsov, and co-workers.¹⁶ This model has been experimentally verified for similar Os complexes tethered by Au–N^{2,13,18} or Au–S¹⁵ and for other redox couples.¹⁹ In the low- E_{bias} and overvoltage (η) limit with sufficient molecule–electrode coupling (the adiabatic limit), the two-step ET formalism predicts that the junction ET current depends on E_{bias} as described by eq 1:

$$I = \kappa \rho (eE_{bias}) \frac{\bar{\omega}}{2\pi} \left\{ \exp \left[\frac{e}{4\lambda kT} (\lambda + \xi \eta + \gamma E_{bias})^2 \right] + \exp \left[\frac{e}{4\lambda kT} (\lambda + E_{bias} - \xi \eta - \gamma E_{bias})^2 \right] \right\}^{-1} \quad (1)$$

where e is the elementary charge, κ is the electronic transmission coefficient, ρ is the density of electronic states in the metal near the Fermi level, k is the Boltzmann constant, and T is the temperature. ξ and γ are model parameters that describe the shift of the effective electrode potential at the redox center with the variation of η and E_{bias} , respectively; they account for the nonlinear potential distribution in the tunneling gap and range between 0 and 1. Equation 1 was derived assuming that κ and ρ have the same values for the substrate–molecule and molecule–tip ETs, respectively. From eq 1, the location of the maximum in I_T is predicted to be

$$E_{max} = E^\circ + (\lambda/2 - \gamma) \frac{E_{bias}}{\xi} \quad (2)$$

Applying the “numerical” version of eq 1 used by Pobelov et al.¹⁹ allows the experimental I_T versus E_S curves to be fitted for both systems (Figure 2, red lines). These theoretical lines were obtained using the fit parameter values $\gamma = 1$, $\xi = 1$ (fixed), and $\lambda = 0.3$ eV for both the Au–C and Au–S systems. A linear dependence of E_{max} on E_{bias} is expected from eq 2 and was experimentally verified for both the Au–S and Au–C bonds in the present study (Figure 2 right). It should be noted that at $E_{bias} = 0$, $E_{max} \approx E^\circ$, as expected from the theory (eq 2). The average slope of the E_{max} vs E_{bias} plots in Figure 2 for both the Au–S and Au–C systems in both the positive- and negative-going E_S scans is roughly -0.6 , which is close to the previously reported value of -0.5 .^{2,19} These observations are consistent with a two-step sequential electrochemical ET mechanism involving the redox levels in the Os complex and the negatively and positively biased electrodes.²⁰

In conclusion, the Au–C- and Au–S-tethered Os complex systems in the STM “tunneling” gap configuration show similar ET mechanisms, namely, two-step ET between the molecule and the contacts (tip and substrate) with partial vibrational relaxation. Similar results have been reported previously for Os complexes tethered by pyridine N to Au and Pt² in aqueous electrolyte and bis(terpyridine)osmium with thiol linkers in ionic liquids but not for Au–C contacts. This demonstrates that molecular wires can be linked directly to Au through a C linkage while still retaining their molecular electronics and electrochemical functionality, as demonstrated here through the gated electrochemical transistor behavior.

Acknowledgment. R.J.N. thanks EPSRC for funding under Grants EP/C00678X/1 and EP/D035678/1. E.J.C. thanks ANPCyT (Argentina) for funding via Grant PICT 2006 N° 1146. A.M.R. acknowledges a Research Studentship from CONICET.

Supporting Information Available: Experimental details and supporting tables and figures. This material is available free of charge via the Internet at <http://pubs.acs.org>.

References

- (1) Tao, N. J. *Phys. Rev. Lett.* **1996**, *76*, 4066.
- (2) Albrecht, T.; Moth-Poulsen, K.; Christensen, J. B.; Guckian, A.; Bjørnholm, T.; Vos, J. G.; Ulstrup, J. *Faraday Discuss.* **2006**, *131*, 265.
- (3) Kubatkin, S.; Danilov, A.; Hjort, M.; Cornil, J.; Brédas, J.-L.; Stühr-Hansen, N.; Hedegård, P.; Bjørnholm, T. *Nature* **2003**, *425*, 698. Reed, M. A.; Zhou, C.; Muller, C. J.; Burgin, T. P.; Tour, J. M. *Science* **1997**, *278*, 252. Cui, X. D.; Primak, A.; Zarate, X.; Tomfohr, J.; Sankey, O. F.; Moore, A. L.; Moore, T. A.; Gust, D.; Harris, G.; Lindsay, S. M. *Science* **2001**, *294*, 571.
- (4) Xu, B. Q.; Tao, N. J. *Science* **2003**, *301*, 1221.
- (5) McCreery, R. L.; Viswanathan, U.; Kalakodimi, R. P.; Nowak, A. M. *Faraday Discuss.* **2006**, *131*, 33. Ranganathan, S.; Steidel, I.; Anariba, F.; McCreery, R. L. *Nano Lett.* **2001**, *1*, 491.
- (6) Tao, N. J. *Nat. Nanotechnol.* **2006**, *1*, 173.
- (7) Chen, F.; Huang, Z.; Tao, N. *Appl. Phys. Lett.* **2007**, *91*, 162106.
- (8) Kiguchi, M.; Miura, S.; Hara, K.; Sawamura, M.; Murakoshi, K. *Appl. Phys. Lett.* **2007**, *91*, 053110. Park, Y. S.; Whalley, A. C.; Kamenetska, M.; Steigerwald, M. L.; Hybertsen, M. S.; Nuckolls, C.; Venkataraman, L. *J. Am. Chem. Soc.* **2007**, *129*, 15768.
- (9) Chen, F.; Li, X.; Hihath, J.; Huang, Z.; Tao, N. *J. Am. Chem. Soc.* **2006**, *128*, 15874. Haiss, W.; Martin, S.; Leary, E.; van Zalinge, H.; Higgins, S. J.; Bouffier, L.; Nichols, R. J. *J. Phys. Chem. C* **2009**, *113*, 5823. Donhauser, Z. J.; Mantooth, B. A.; Kelly, K. F.; Bumm, L. A.; Monnell, J. D.; Stapleton, J. J.; Price, D. W.; Rawlett, A. M.; Allara, D. L.; Tour, J. M.; Weiss, P. S. *Science* **2001**, *292*, 2303.
- (10) Allongue, P.; Delamar, M.; Desbat, B.; Fagebaume, O.; Hitmi, R.; Pinson, J.; Saveant, J.-M. *J. Am. Chem. Soc.* **1997**, *119*, 201. Adenier, A.; Bernard, M.-C.; Chehimi, M. M.; Cabot-Deliry, E.; Desbat, B.; Fagebaume, O.; Pinson, J.; Podvorica, F. *J. Am. Chem. Soc.* **2001**, *123*, 4541. Laforge, A.; Addou, T.; Belanger, D. *Langmuir* **2005**, *21*, 6855. Ricci, A.; Bonazzola, C.; Calvo, E. *J. Phys. Chem. Phys.* **2006**, *8*, 4297.
- (11) Strano, M. S.; Dyke, C. A.; Usrey, M. L.; Barone, P. W.; Allen, M. J.; Shan, H.; Kittrell, C.; Hauge, R. H.; Tour, J. M.; Smalley, R. E. *Science* **2003**, *301*, 1519.
- (12) Liu, G. Z.; Liu, J. Q.; Bocking, T.; Eggers, P. K.; Gooding, J. J. *Chem. Phys.* **2005**, *319*, 136. Adenier, A.; Cabot-Deliry, E.; Chaussé, A.; Griveau, S.; Mercier, F.; Pinson, J.; Vautrin-UI, C. *Chem. Mater.* **2005**, *17*, 491. Bernard, M.-C.; Chaussé, A.; Cabot-Deliry, E.; Chehimi, M. M.; Pinson, J.; Podvorica, F.; Vautrin-UI, C. *Chem. Mater.* **2003**, *15*, 3450.
- (13) Albrecht, T.; Guckian, A.; Ulstrup, J.; Vos, J. G. *Nano Lett.* **2005**, *5*, 1451.
- (14) Albrecht, T.; Guckian, A.; Ulstrup, J.; Vos, J. G. *IEEE Trans. Nanotechnol.* **2005**, *4*, 430.
- (15) Albrecht, T.; Moth-Poulsen, K.; Christensen, J. B.; Hjelm, J.; Bjørnholm, T.; Ulstrup, J. *J. Am. Chem. Soc.* **2006**, *128*, 6574.
- (16) Kuznetsov, A. M.; Ulstrup, J. *J. Phys. Chem. A* **2000**, *104*, 11531. Zhang, J.; Chi, Q.; Kuznetsov, A. M.; Hansen, A. G.; Wackerbarth, H.; Christensen, H. E. M.; Andersen, J. E. T.; Ulstrup, J. *J. Phys. Chem. B* **2002**, *106*, 1131. Zhang, J.; Chi, Q.; Albrecht, T.; Kuznetsov, A. M.; Grubb, M.; Hansen, A. G.; Wackerbarth, H.; Welinder, A. C.; Ulstrup, J. *Electrochim. Acta* **2005**, *50*, 3143.
- (17) Ricci, A.; Rolli, C.; Rothacher, S.; Baraldo, L.; Bonazzola, C.; Calvo, E.; Tognalli, N.; Fainstein, A. *Solid State Electrochem.* **2007**, *11*, 1511.
- (18) Albrecht, T.; Guckian, A.; Kuznetsov, A. M.; Vos, J. G.; Ulstrup, J. *J. Am. Chem. Soc.* **2006**, *128*, 17132.
- (19) Pobelov, I. V.; Li, Z.; Wandlowski, T. *J. Am. Chem. Soc.* **2008**, *130*, 16045.
- (20) Kuznetsov, A. M.; Ulstrup, J. *J. Phys. Chem. A* **2001**, *105*, 7494. Zhang, J.; Kuznetsov, A. M.; Medvedev, I. G.; Chi, Q.; Albrecht, T.; Jensen, P. S.; Ulstrup, J. *J. Chem. Rev.* **2008**, *108*, 2737.

JA907867B